Special Issue on "Theoretical and Computational Chemistry"

J. Indian Chem. Soc.,
Vol. 96, July 2019, pp. 837-844

Chemical reactivity profile and bonding nature of cadmium chalcogenides fullerene

Debolina Paul, Jyotirmoy Deb and Utpal Sarkar*

Department of Physics, Assam University, Silchar-788 011, Assam, India

E-mail: utpalchemiitkgp@yahoo.com

Manuscript received online 23 April 2019, revised and accepted 15 May 2019

We present a detailed density functional theory study on the structural properties, chemical reactivity parameters and bonding analysis of cadmium chalcogenide fullerenes ($Cd_{12}X_{12}$, X = S, Se, Te) and compared them to their pristine counterpart, C_{24}. The energetic stability via cohesive energy per atom indicates that the fullerenes are stable. Bond length elongation occurs on $Cd_{12}X_{12}$ with increasing atomic size from S to Te. $Cd_{12}Te_{12}$ shows high redox characteristic with the lowest ionization potential and highest electron affinity values. All these fullerenes can be used as UV light protectors. Lastly, to get insight into the nature of bonding character, here we performed bonding analysis based on Wiberg bond index and electron density analysis of these fullerenes.

Keywords: Density functional theory, pristine and cadmium chalcogenide fullerenes, chemical reactivity parameters, bonding analysis.

Introduction

Fullerenes[1] or hollow nanocages are interesting for the possible large range of their applications in various fields. It has been a subject of interest to the researchers worldwide for its fascinating properties as well. For instance, the internal cavity of these nanomaterials offers opportunity to host other elements or small clusters, behaving as sensors or as storage devices[2,3]. They are widely used as photovoltaic devices[4], molecular switches[5] and in spintronics application[6]. Fullerenes or hollow nanostructures are also explored for their applications in photocatalysis[7], in the field of medical science, such as development of artificial cells[8], delivery of drugs[8,9], as an antioxidant[10], as an anticancer agent[10], protection of biologically active agents such as proteins[8], enzymes or DNAs[8], for imaging purpose[9,10], radio therapy[9,10] and so on. And it has been found that doping induces various changes in all the above mentioned properties and applications. The presence of any foreign atom shows significant influence on the electronic, optical and nonlinear optical properties of the fullerenes[11–17]. Fullerene C_{24} is considered as the smallest one which is composed of four and six-membered rings among all different fullerenes[14].

Over the past couple of years, compound materials which fall in the II-VI group of the periodic table are of great interest to semiconductor industry, since they find their potential technological applications such as photovoltaic devices, quantum devices, sensors, visible light driven photocatalysis, optical sensitizers, in solar cells etc.[18–21]. These type of semiconductor nanomaterials also find their usage in light emitting diodes (LEDs), thin film transistors[22,23] and many more. Among these, the cadmium chalcogenide semiconductors (II-VI group) have received significant attention and are extensively researched owing to their outstanding optical and electronic properties[24,25]. They show multiple exciton generation, large extinction coefficient and size dependent tunability of the optical and electronic properties[26,27]. Either as one/two dimensional, or as quantum dots or as clusters, the cadmium chalcogenides are extensively studied. For instance, the visible range of the CdS and CdSe quantum dots can be tuned simply by changing their size and also by their experimental preparation methods[28]. Moreover, the CdX quantum dots have good potential in optoelectronic devices[29], which is due to their superior optical properties including narrow emission, high photostability and broad absorption. Cd_nS_n cluster (n = 1-8) finds their application in the field of nonlinear optics[30]. CdSe quantum dots are considered as excellent photoluminescence emitters of blue light[31]. Apart from quantum dots, clusters and core-shell structures, the

2D structure of CdX are also immensely used for designing of novel materials[20,32,33].

To understand these cadmium chalcogenides, it is necessary to gain insight into their structural, electronic, optical properties, thereby acquiring more knowledge to enhance their applicability in different fields. Although a number of theoretical studies on bulk system have been reported about their electronic structure, a few works is mentioned in the literature on their clusters[30]. Hence, there lies a gap to research more on their behavior as small clusters or fullerenes. In addition, study on their clusters could be helpful to know about their local properties, which are otherwise unseen in their bulk form, and includes their catalytic behavior also.

In this work, we have considered studying the structural parameters of cadmium chalcogenides along with their electronic and chemical reactivity descriptors. We have also provided a brief study on the nature of bonding of their bond, with the help of electron density analysis. Furthermore, a study on their absorption spectra has been speculated. Finally, a brief comparison of these CdX (X = S, Se, Te) fullerenes are done with their pristine C_{24} counterpart.

Computational techniques

The electronic structure calculations have been performed within the framework of density functional theory (DFT). We have used meta exchange-correlation hybrid functional (M06-2X)[34] as implemented in Gaussian 09 program package[35]. All electron (AE) triple zeta valence basis set along with heavily polarized and diffuse functional def2TZVPPD[36] is used for the calculation. For Cd and Te atoms effective core potential (ECP) is also considered. No symmetry restriction is imposed during structure optimization. Frequency calculations are used to verify the nature of the saddle points. The local minima of these structures in the potential energy landscape is confirmed due to presence of only real frequencies. The time-dependent density functional theory (TDDFT) calculations are also performed at the same level of theory as that of geometry optimization to achieve the crucial excited states of the related structures. Topological analysis of the electron density, at bond critical points, has been performed using Multiwfn software[37] in the context of Bader's atoms in molecules (AIM) theory[38]. Density of states (DOS) and absorption spectra analysis are carried out with the help of GaussSum program[39].

The adiabatic ionization potential (AIP) and the adiabatic electron affinity (AEA) of the fullerenes are calculated using the formulae:

$$AIP = E(N-1) - E(N) \quad (1)$$

$$AEA = E(N) - E(N+1) \quad (2)$$

where, $E(N-1)$, $E(N)$ and $E(N+1)$ are the respective energies of the $(N-1)$, N and $(N+1)$ electron systems.

Chemical reactivity descriptors[40] namely, chemical hardness (η)[41], chemical potential (μ) and electrophilicity index (ω)[42,43] for all the systems are obtained using the following equations:

$$\eta = AIP - AEA \quad (3)$$

$$\mu = -\frac{(AIP + AEA)}{2} \quad (4)$$

$$\omega = \frac{\mu^2}{2\eta} \quad (5)$$

Results and discussion

The optimized geometries of the studied cadmium chalcogenide fullerenes along with their pristine counterpart, fullerene C_{24} is depicted in Fig. 1. Though C_{24} fullerene possesses two different types of symmetric structures, the

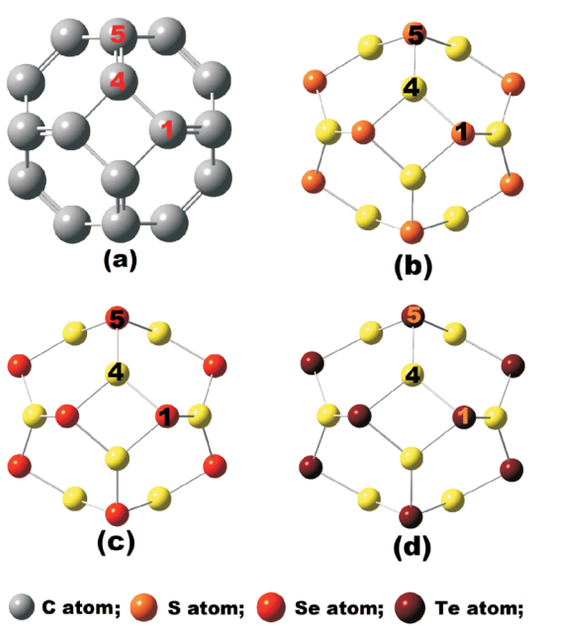

Fig. 1. Optimized geometries of (a) C_{24}, (b) $Cd_{12}S_{12}$, (c) $Cd_{12}Se_{12}$ and (d) $Cd_{12}Te_{12}$.

present study focuses on the D_{6d} symmetry of fullerene C_{24}[44] because its substitutional doping with 12 X and 12 Y atoms converts it to T_h symmetry, which is highly symmetric. But fullerene C_{24}, as well as the doped structures ($Cd_{12}X_{12}$, X = S, Se, Te), both contain eight six-membered rings which are isolated by six four-membered rings. All the bonds present in the tetragon are mimicking each other. Similarly, in case of hexagon, three bonds are contributing from tetragon and the environment of remaining three bonds are same. Thus, for simplicity, we consider only one bond 4(C/Cd)-5(C/X) from tetragon and one bond 1(C/X)-4(C/Cd) from hexagon for the purpose of structural and bonding analysis.

Energetic stability

The cohesive energy per atom (CE) of these systems have been computed in order to investigate the energetic stability and is given by the equation[14,45,46],

$$CE = \frac{E_{system} - [nE_P + mE_Q]}{n + m} \quad (6)$$

where, E_{system} is the total energy of the fullerene C_{24} or $Cd_{12}X_{12}$, E_P and E_Q are total energies of P (= C/Cd) and Q (= C/S/Se/Te) atoms respectively. Here, n and m are respectively the number of P and Q atoms mentioned above.

Cohesive energy is regarded as one of the important parameters to understand the trend in the formation of fullerene molecules. The negative CE values of the fullerenes confirm that they are stable and it would be difficult to break them spontaneously into their constituent atoms. Fullerene C_{24} (–8.055 eV) is obviously more stable than cadmium chalcogenide fullerenes, with the highest CE value. Among the CdX fullerenes, the stability decreases with increase in size of the chalcogenide atoms, i.e. $Cd_{12}S_{12}$ (–3.102 eV) > $Cd_{12}Se_{12}$ (–2.857 eV) > $Cd_{12}Te_{12}$ (–2.395 eV).

Structural properties

As soon as the D_{6d} symmetry of pristine C_{24} changes to T_h on account of doping (by 12 Cd and 12 X atoms), their structures also change drastically, causing a change in their bond lengths and bond angles. We have provided a detailed discussion on the changes acquired by some of the bond lengths and bond angles (Table S1 of Supporting Information) of all the systems. By checking carefully, the basic structural features of these fullerenes, it is observed that the bond distances connecting any two atoms in a tetragon (4-5) and a hexagon (16-15) are very similar, but the bonds in the hexagonal atoms are substantially smaller than the tetragonal atoms. The bond length of pristine C_{24} stretches when doping is introduced. And as expected the bond length of $Cd_{12}X_{12}$ fullerenes, elongates as the atomic radius of the chalcogenide atom increases down the group from S to Te. Also, one more interesting point to be noted is that not only the Cd-X bond lengths of $Cd_{12}X_{12}$ increases, with respect to the C-C bonds in C_{24}, but the double bonds present in C_{24} are also converted to single bonds with doping. This may be due to the change of hybridization from sp^2 to sp^3, that the double bonds are saturated to singles and increment in the bond distances occur in $Cd_{12}X_{12}$ fullerenes as compared to C_{24}. Now in case of the bond angles, we find that all the angles in the tetragon of C_{24} are right angles. However, in $Cd_{12}X_{12}$, the tetragonal angles, 4(Cd)-1(X)-2(Cd) and 3(X)-4(Cd)-1(X) follow a decreasing and increasing trend respectively as we move from S to Te atoms. The bond angles, 5-4-1 and 4-1-14, which are 120° for C_{24}, increases from $Cd_{12}S_{12}$ < $Cd_{12}Se_{12}$ < $Cd_{12}Te_{12}$ for the former one, while it decreases for the latter one following the same sequence.

Chemical reactivity descriptors

Chemical reactivity parameters are not only useful to analyze the reactivity but also to study the reaction pathway mechanism[47]. Besides, these parameters describe toxicity and some excited state phenomenon[48,49]. The energy gap (E_g), mathematically obtained from the difference of highest occupied molecular orbital (HOMO) and lowest unoccupied molecular orbital (LUMO) is an indicator of chemical stability of any system. To polarize a system with low energy gap is easier and this makes it more reactive as compared to hard ones, since it can easily offer electrons to an acceptor. The chemical reactivity descriptors are listed in Table 1. From the E_g values of fullerenes, one may observe that the energy gap of C_{24} is lowest as compared to $Cd_{12}X_{12}$ fullerenes. However, with the increasing size of the X atom (S > Se > Te), E_g value is found to come down gradually. In other words, the sulphur doped fullerene ($Cd_{12}S_{12}$) possess the highest E_g among all the fullerenes. The energy gap of all these fullerenes fall in the UV region, which may be suitable for UV light protectors. Lower value of ionization potential (AIP) specifies that a system is easier to oxidize. Ionization potential of the CdX fullerene decreases as $Cd_{12}S_{12}$ > $Cd_{12}Se_{12}$ > $Cd_{12}Te_{12}$, while the opposite is true in case of electron affin-

Table 1. Chemical reactivity descriptors of C_{24} and $Cd_{12}X_{12}$ (X = S, Se, Te) fullerenes

Fullerenes	E_g (eV)	Φ (eV)	AIP (eV)	AEA (eV)	η (eV)	μ (eV)	ω (eV)
C_{24}	4.472	5.161	8.087	2.304	5.783	–5.196	2.334
$Cd_{12}S_{12}$	5.482	5.433	8.551	2.502	6.049	–5.527	2.525
$Cd_{12}Se_{12}$	5.136	5.347	8.319	2.579	5.740	–5.449	2.586
$Cd_{12}Te_{12}$	4.635	5.122	7.791	2.584	5.207	–5.188	2.585

ity (AEA). Hence the redox characteristic of these fullerenes may be tuned. In the present work, chemical hardness (η) and energy gap (E_g) correlate each other, i.e. they follow same trend. Also, $Cd_{12}S_{12}$ has the highest adiabatic ionization potential and lowest adiabatic electron affinity among the $Cd_{12}X_{12}$ fullerenes. Chemical potential (μ) of any system is a measure of the escaping tendency of its electron cloud which in turn implies that a system with higher chemical potential possesses greater tendency of losing the electron cloud from itself. Chemical potential of $Cd_{12}S_{12}$ is the highest. Electrophilicity index (ω) provides information related to kinetic and thermodynamic properties of a system. It depends not only on chemical hardness but also on chemical potential of any system. Among the $Cd_{12}X_{12}$ fullerenes, $Cd_{12}S_{12}$ is the least electrophilic.

The work function of a system is defined as the least amount of energy required to remove an electron from the Fermi level to a point far enough. The change of work function of a material due to various perturbation applied to it alters its field emission properties. One may notice that the work function (Φ) of pristine C_{24} is not much altered due to doping. Interestingly after the substitution of all carbon atoms by cadmium and tellurium atoms in $Cd_{12}Te_{12}$ fullerene, the work function decreases slightly and probably it has the least chemical hardness among the fullerenes. This indicates that the conductance of $Cd_{12}Te_{12}$ increases with decrease in the work function, as compared to pristine C_{24}.

Density of states

The total density of states (TDOS) and projected density of states (PDOS) of pristine C_{24} and $Cd_{12}X_{12}$ (X = S, Se, Te) fullerenes have been plotted in Fig. 2. There are no states present near the Fermi level of the systems, confirming that they are semiconductors. Even with doping on pristine C_{24}, the semiconducting nature remains unaltered. In case of $Cd_{12}X_{12}$ fullerenes, it is clear that in our considered energy range, i.e. between –12 eV to 4 eV, the dominant contribution to the total DOS is coming from the X atom. The LUMO energy level of the $Cd_{12}X_{12}$ fullerenes is however primarily contributed by the Cd atom. In the conduction band (CB) region of the doped fullerenes, prominent energy states of the X atoms in each of the cadmium chalcogenide fullerenes starts at around 0 eV onwards. The HOMO energy level, on the other hand, is taken over by the X atom in each of the $Cd_{12}X_{12}$ fullerenes. Hence, from the DOS analysis, one may come to a conclusion that, although the energy states corresponding to the X atoms are dominant in the energy window taken here, still, Cd atom finds a prominent place when it comes in the CB region and dictates the energy state of the LUMO level.

Absorption spectra

To study the electronic transitions of pristine C_{24} and its substituted cadmium derivatives, $Cd_{12}X_{12}$ (X = S, Se, Te) fullerenes, we have performed time-dependent density functional theory (TDDFT) calculations. The maximum absorption wavelength corresponding to the highest oscillator strength and the major electronic transitions of the fullerenes are provided in Table S2 of Supporting Information and the corresponding spectra are depicted in Fig. 3. Doping in pristine fullerene induces change not only in the oscillation strength but also in the amplitude and position of the highest absorption peak. In case of C_{24}, the major electronic transition is located at 294.555 nm with the most relevant contribution coming from HOMO to LUMO+4 (68%), leading to an oscillator strength of 0.0604. But, for the cadmium derivatives, the situation changes. For $Cd_{12}S_{12}$ and $Cd_{12}Se_{12}$, the main contributions come from HOMO-12 to LUMO (76%) and HOMO-3 to LUMO+1 (71%) with the highest electronic transitions absorbing at 294.892 nm and 308.902 nm respectively. It is worth noting that the oscillator strength is considerably increased to 0.1117 and 0.6662 respectively for $Cd_{12}S_{12}$ and $Cd_{12}Se_{12}$, with respect to C_{24}. However, $Cd_{12}Te_{12}$ records a much smaller oscillator strength of 0.0030 as compared to the other fullerenes, thus significantly lowering the amplitude of the maximum absorption peak (351.858

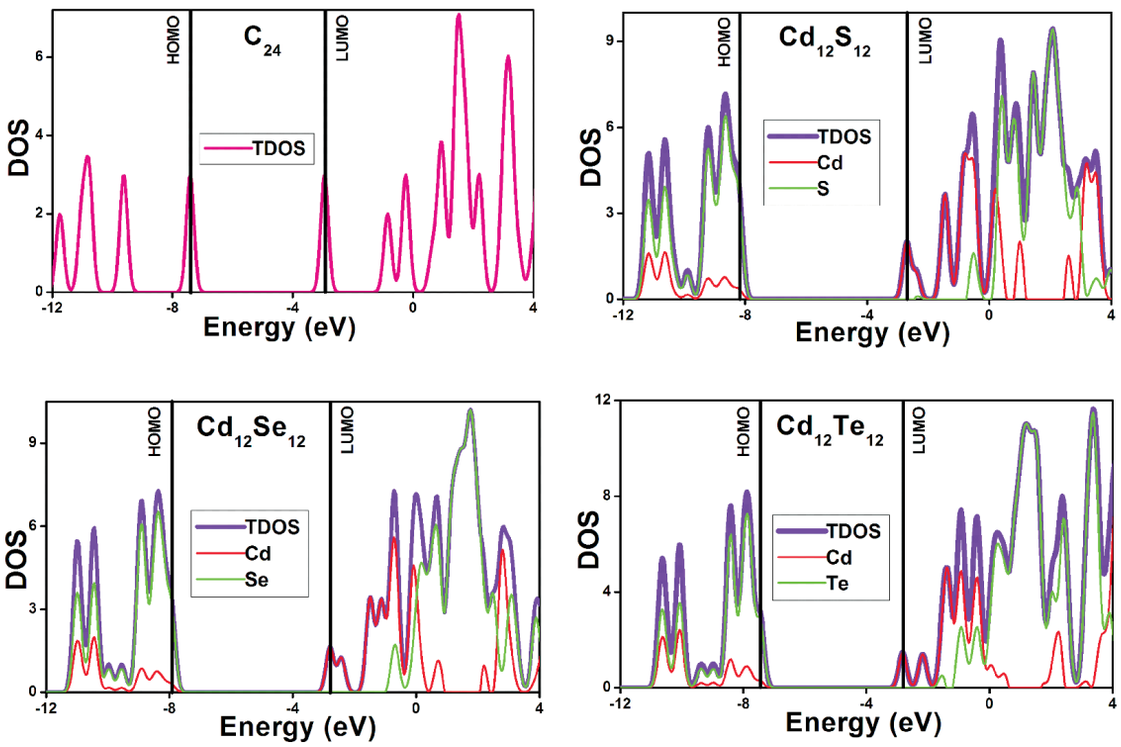

Fig. 2. Total density of states (TDOS) and the projected density of states (PDOS) of pristine C_{24} and $Cd_{12}X_{12}$ (X = S, Se, Te) fullerenes.

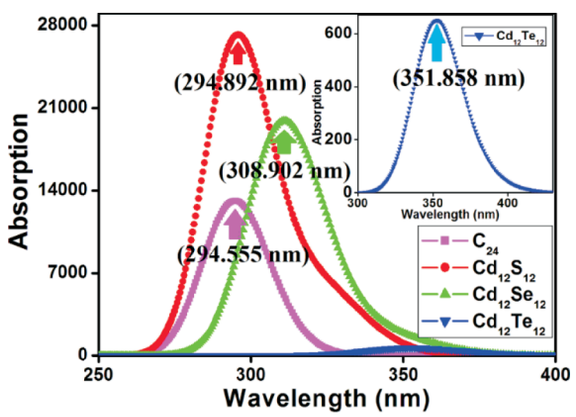

Fig. 3. UV-Visible absorption spectra of C_{24} and $Cd_{12}X_{12}$ (X = S, Se, Te) fullerenes.

nm); and for this system, crucial electronic transitions take place from HOMO-11 to LUMO (89%). The reduction in the oscillator strength of $Cd_{12}Te_{12}$ fullerene may be due to its lower value of transition dipole moment, which ultimately puts an impact on the intensity of the highest electronic transition. It can be observed that the highest absorption peak of the fullerenes is located in between 294 nm to 352 nm. Hence, all the fullerenes are good absorber in the UV region and can be used in designing UV light protection devices. In addition, one may also note that the peak corresponding to maximum absorption of the doped fullerenes move towards the longer wavelength region in comparison to C_{24} and the highest shift is found for $Cd_{12}Te_{12}$ fullerene.

Bonding analysis

To get a clear idea about nature of bonding, here we performed Wiberg bond index (WBI)[50] and electron density analysis (EDA)[38] on the aforesaid bonds considered in the present study. The WBI is reported in Table S3 of Supporting Information. The magnitude of WBI provides information regarding the extent of covalent character of a particular bond[51]. The magnitude of WBI of the selected bonds of pristine C_{24} shows that both these bonds have covalent character. Depending on the magnitude of WBI, we can infer whether a bond is a single bond or a double bond. If WBI is near to one, then it referred to as a single bond and if it is higher than one then it is a double bond. Thus WBI value of C_{24} suggest that C4-C1 is a single bond whereas C4-C5 is a double bond and this is in good agreement with Fig. 1(a). The higher value of

Table 2. Electron density descriptors (in a.u.) at the bond critical points (BCPs) in between some selected bonds of C_{24} and $Cd_{12}X_{12}$ (X = S, Se, Te) fullerenes

Fullerenes	BCP	$\rho(r_c)$	$\nabla^2\rho(r_c)$	$G(r_c)$	$V(r_c)$	$H(r_c)$	$-G(r_c)/V(r_c)$	$G(r_c)/\rho(r_c)$
C_{24}	C(4)-C(5)	0.259	–0.625	0.079	–0.314	–0.235	0.252	0.305
	C(1)-C(4)	0.334	–0.995	0.125	–0.499	–0.374	0.251	0.374
$C_{12}S_{12}$	Cd(4)-S(5)	0.055	0.134	0.044	–0.054	–0.010	0.815	0.800
	S(1)-Cd(4)	0.067	0.158	0.055	–0.071	–0.016	0.775	0.821
$C_{12}Se_{12}$	Cd(4)-Se(5)	0.049	0.102	0.035	–0.044	–0.009	0.795	0.714
	Se(1)-Cd(4)	0.060	0.117	0.043	–0.056	–0.013	0.768	0.717
$C_{12}Te_{12}$	Cd(4)-Te(5)	0.043	0.070	0.026	–0.034	–0.008	0.765	0.605
	Te(1)-Cd(4)	0.051	0.075	0.030	–0.042	–0.011	0.714	0.588

WBI of C4-C5 bond than C4-C1 bond also reflects that the electron rich bond is localized between tetragons whereas hexagonal rings are electron deficient. Interestingly, in case of $Cd_{12}X_{12}$ (X = S, Se, Te) fullerenes WBI values decrease significantly for the considered bonds indicating a decrease of the degree of covalency. Though the bonds here are single order, but not fully covalent in nature. Among the doped structures, $C_{12}Te_{12}$ shows more covalent character than others. For a particular structure, hexagonal bonds are more covalent than tetragonal bonds and the extent of covalent character increases following the trend $Cd_{12}S_{12} < Cd_{12}Se_{12} < Cd_{12}Te_{12}$.

More insight into the nature of C/Cd-C/X (X = S, Se, Te) bonding can be obtained from electron density analysis. The topological descriptors at bond critical points (BCPs) are provided in Table 2. The presence of covalent and non-covalent interactions can be determined from the negative and positive values of Laplacian of electron density ($\nabla^2\rho_{BCP}$) at BCPs which indicates concentration and depletion of electron density at BCPs. Usually, a low value of electron density ($\rho(r_c)$) and positive value of ($\nabla^2\rho(r_c)$) indicate a closed-shell type bonding whereas a high value of electron density ($\rho(r_c)$) and negative value of ($\nabla^2\rho(r_c)$) represent strong covalent type of interaction[52]. But for the systems with 3d orbitals or heavier atoms, only considering ($\nabla^2\rho(r_c)$) is not sufficient to describe the nature of bonding. In that case we have to consider some more parameter like local kinetic energy density ($G(r_c)$), local potential energy density ($V(r_c)$), local electron energy density ($H(r_c)$) and the ratio of $-G(r_c)/V(r_c)$ and $G(r_c)/(\rho(r_c)$. The local electron energy density (H_{BCP}) can be calculated using the relation:

$$H(r_c) = G(r_c) + V(r_c) \quad (7)$$

Based on the above topological descriptors Cremer and coworkers[53] classified other types of interaction such as if $\nabla^2\rho(r_c) > 0$ and $H(r_c) < 0$ than the nature of bonding is partially covalent type. Further, if the value of $-G(r_c)/V(r_c)$ lies between 0.5 and 1 then there exist some degree of covalent character (partial covalent type) and if $-G(r_c)/V(r_c) > 1$ indicates a purely noncovalent type of interaction. In order to get more information about the covalent nature the role of the ratio $G(r_c)/\rho(r_c)$ is taken into consideration. The magnitude of $G(r_c)/\rho(r_c) < 1$ clearly confirms some degree of covalent nature of the considered bonds.

Fig. 4 represents the contour plot showing the Laplacian of electron density ($\nabla^2\rho(r_c)$) at BCPs**.** Depletion of charge density (i.e. $\nabla^2\rho(r_c) > 0$) is represented by green-coloured

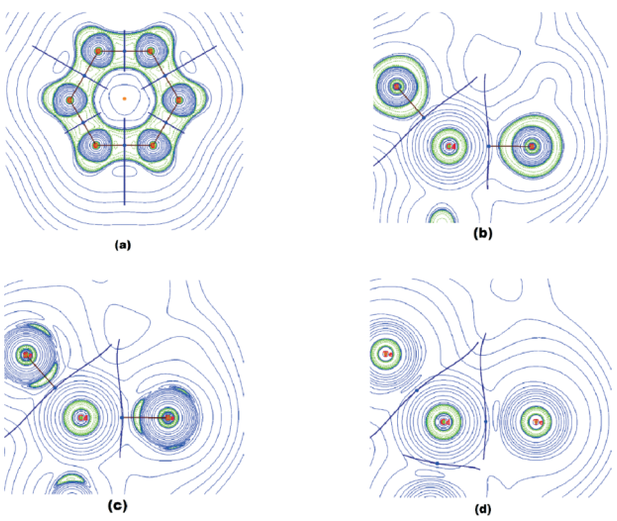

Fig. 4. Contour plot of Laplacian of electron density at a particular plane of (a) C_{24}, (b) $Cd_{12}S_{12}$, (c) $Cd_{12}Se_{12}$ and (d) $Cd_{12}Te_{12}$ fullerenes. Blue colour portion stand for $\nabla^2\rho(r_c) > 0$ whereas, green colour portion represents $\nabla^2\rho(r_c) < 0$.

portion while the blue-coloured represents accumulation of charge density (i.e. $\nabla^2\rho(r_c) < 0$). The bond paths and inter-atomic surfaces of corresponding bonds are also shown. Both the bonds of pristine C_{24} are purely covalent in nature as it satisfies the condition $\nabla^2\rho(r_c)$ and $H(r_c)$ both are negative. Also the ratios $-G(r_c)/V(r_c)$ and $G(r_c)/\rho(r_c)$ confirms the covalent nature of these bonds[51]. However, for $Cd_{12}X_{12}$ (X = S, Se, Te) fullerenes all the considered bonds under study are of partial covalent type as $\nabla^2\rho(r_c) > 0$ and $H(r_c) < 0$. As the $-G(r_c)/V(r_c)$ value of these bonds are lies between 0.5 and 1 and also $G(r_c)/\rho(r_c) < 1$ which again confirms the partial covalent nature of these bonds[54]. The topological descriptors $\nabla^2\rho(r_c)$, $-G(r_c)/V(r_c)$ and $G(r_c)/\rho(r_c)$ decreases in the manner $Cd_{12}S_{12} < Cd_{12}Se_{12} < Cd_{12}Te_{12}$ implies the increment of covalent character among these bonds as we move from $Cd_{12}S_{12}$ to $Cd_{12}Te_{12}$. Importantly, the results of WBI supports the results of EDA.

Conclusion

Structural properties, chemical reactivity parameters and bonding analysis of C_{24} and $Cd_{12}X_{12}$ (X = S, Se, Te) fullerenes have been presented based on DFT calculations. All the fullerenes are energetically stable confirmed by their negative values of cohesive energy. Doping by Cd and X atoms initiates increment in the bond distances of the C-C bonds in C_{24}. With the increasing size of the atomic radii of the X atoms, the bond lengths are also found to increase. The bond angles are also affected. The energy gap and chemical hardness which correlates each other also shows a monotonic decrease from S to Te atom in $Cd_{12}X_{12}$ fullerenes. Ionization potential also follows the same trend. However, the electron affinity and chemical potential of $Cd_{12}X_{12}$ increases as we walk down the group VI (i.e. S < Se < Te). Since there is a change in the ionization potential and electron affinity of these fullerenes, hence there is a chance of tuning their redox characteristics, with $Cd_{12}Te_{12}$ leading the list with the lowest AIP and highest AEA value. The UV-Visible absorption spectra show that the highest peak corresponding to the highest oscillator strength of the CdX fullerenes shifts towards the higher wavelength region (red-shifted) in comparison to C_{24} and also with the increasing atomic radius from S to Te. All the fullerenes absorb in the UV region and are applicable in UV light protection devices. Bonding analysis tells that considered bonds for C_{24} fullerene is purely covalent in nature. However, for $Cd_{12}X_{12}$ (X = S, Se, Te) fullerenes the same bonds are showing partly covalent character but the extent of covalency increases as the size of the X (S, Se, Te) atom increases.

Acknowledgement

Authors dedicate this work to celebrate the 60th birthday of Professor P. K. Chattaraj. DP thanks University Grants Commission, India for her fellowship. JD thanks, Department of Science and Technology, India for the INSPIRE fellowship. US would like to thank DST, New Delhi, India for the SERB project for financial assistance (File No. EMR/2016/006764).

Supporting Information

Supporting Information related to this article is provided in the “Supporting_Information.docx” file.

References

1. H. W. Kroto, J. Heath, S. C. O’Brien, R. F. Curl and R. E. Smalley, *Nature*, 1985, **318**, 162.
2. O. V. Pupysheva, A. A. Farajian and B. I. Yakobson, *Nano Lett.*, 2008, **8**, 767.
3. S. A. Siadatia, E. Vessallyb, A. Hosseinianc and L. Edjlali, *Synth. Met.*, 2016, **220**, 606.
4. A. Mohajeri and A. Omidvar, *Phys. Chem. Chem. Phys.*, 2015, **17**, 22367.
5. B. Wu, T. S. Wang, Y. Q. Feng, Z. X. Zhang, L. Jiang and C. R. Wang, *Nat. Commun.*, 2015, **6**, 6468.
6. J. Wang, Y. Liu and Y.-C. Li, *Phys. Chem. Chem. Phys.*, 2010, **12**, 11428.
7. A. Kh. Vorobiev, R. R. Gazizov, A. Ya. Borschevskii, V. Yu. Markov, V. A. Ioutsi, V. A. Brotsman and L. N. Sidorov, *J. Phys. Chem. A*, 2017, **121**, 113.
8. S. Bhusal, J. A. R. Lopez, J. U. Reveles, T. Baruah and R. R. Zope, *J. Phys. Chem. A*, 2017, **121**, 3486.
9. R. Partha and J. L. Conyers, *Int. J. Nanomedicine*, 2009, **4**, 261.
10. E. Castro, A. H. Garcia, G. Zavala and L. Echegoyen, *J. Mater. Chem. B*, 2017, **5**, 6523.
11. D. Paul, J. Deb, B. Bhattacharya and U. Sarkar, *AIP Conf. Proc.*, 2017, **1832**, 050107(1-3).
12. D. Paul, J. Deb, B. Bhattacharya and U. Sarkar, *Int. J. Nano. Sci.*, 2017, **16**, 1760026(1-5).
13. K. Srinivasu, N. K. Jena and S. K. Ghosh, *AIP Advances*, 2012, **2**, 042111(1-8).
14. D. Paul, J. Deb, B. Bhattacharya and U. Sarkar, *J. Mol. Model.*, 2018, **24**, 204(1-13).

15. S. Bhusal, R. R. Zope, S. Bhatta and T. Baruah, *J. Phys. Chem. C*, 2016, **120**, 27813.
16. D. Paul, B. Bhattacharya, J. Deb and U. Sarkar, *AIP Conf. Proc*., 2018, **1953**, 030236(1-3).
17. L. Wang, J.-T. Ye, H.-Q. Wang, H.-M. Xie and Y.-Q. Qiu, *J. Phys. Chem. C*, 2018, **122**, 6835.
18. X. Zong, H. Yan, G. Wu, G. Ma, F. Wen, L. Wang and C. Li, *J. Am. Chem. Soc*., 2008, **130**, 7176.
19. M. Afzaal and Paul O'Brien, *J. Mater. Chem*., 2006, **16**, 1597.
20. P. Garg, S. Kumar, I. Choudhuri, A. Mahata and B. Pathak, *J. Phys. Chem. C*, 2016, **120**, 7052.
21. S. G. Kumara and K. S. R. K. Rao, *Energy Environ. Sci*., 2014, **7**, 45.
22. M. A. Haase, J. Xie, T. A. Ballen, J. Zhang, B. Hao, Z. H. Yang, T. J. Miller, X. Sun, T. L. Smith and C. A. Leatherdale, *Appl. Phys. Lett*., 2010, **96**, 231116(1-3).
23. X. Duan, C. Niu, V. Sahi, J. Chen, J. W. Parce, S. Empedocles and J. L. Goldman, *Nature*, 2003, **425**, 274.
24. J. Zhou, J. Huang, B. G. Sumpter, P. R. C. Kent, Y. Xie, H. Terrones and S. C. Smith, *J. Phys. Chem. C*, 2014, **118**, 16236.
25. M. Amelia, C. Lincheneau, S. Silvi and A. Credi, *Chem. Soc. Rev*., 2012, **41**, 5728.
26. Z. Lin, A. Franceschetti and M. T. Lusk, *ACS Nano*, 2011, **5**, 2503.
27. K. A. Nguyen, P. N. Day and R. Pachter, *J. Phys. Chem. C,* 2010, **114**, 16197.
28. H.-L. Chou, C.-H. Tseng, K. C. Pillai, B.-J. Hwang and L.-Y. Chen, *J. Phys. Chem. C*, 2011, **115**, 20856.
29. H. Zhang, G. S. Selopal, Y. Zhou, X. Tong, D. Benetti, L. Jin, F. N. Pardo, Z. Wang, S. Sun, H. Zhao and F. Rosei, *Nanoscale*, 2017, **9**, 16843.
30. D. Pegu, J. Deb, D. Paul and U. Sarkar, *Computational Condensed Matter,* 2018, **14**, 40.
31. J. Cho, Y. K. Jung, J.-K. Lee and H.-S. Jung, *Langmuir*, 2017, **33**, 3711.
32. X.-D. Wen, R. Hoffmann and N. W. Ashcroft, *Adv. Mater*., 2013, **25**, 261.
33. J. Deb, D. Paul and U. Sarkar, *AIP Conf. Proc*., 2018, **1953**, 030235(1-5).
34. Y. Zhao and D. G. Truhlar, *Theor. Chem. Account*., 2006, **120**, 215.
35. M. J. Frisch, *et al*., GAUSSIAN 09 (Revision D.01), Gaussian, Inc., Wallingford, CT, 2016.
36. F. Weigend and R. Ahlrichs, *Phys. Chem. Chem. Phys*., 2005, **7**, 3297.
37. T. Lu and F. Chen, *J. Comput. Chem*., 2012, **33**, 580.
38. R. F. W. Bader, Clarendon Press, Oxford, UK, 1990.
39. N. M. O'Boyle, A. L. Tenderholt and K. M. Langner, *J. Comput. Chem*., 2008, **29**, 839.
40. P. K. Chattaraj, "Chemical reactivity theory: A density functional view", Taylor and Francis, CRC Press, Boca Raton, 2009.
41. P. W. Ayers, *Faraday Discuss*., 2007, **135**, 161.
42. R. G. Parr, L. V. Szentpály and S. Liu, *J. Am. Chem. Soc*., 1999, **121**, 1922.
43. P. K. Chattaraj, U. Sarkar and D. R. Roy, *Chem. Rev*., 2006, **106**, 2065.
44. J.-J. Adjizian, A. Vlandas, J. Rio, J.-C, Charlier and C. P. Ewels, *Phil. Trans. R. Soc. A*, 2016, **374**, 20150323(1-18).
45. T. P. Kaloni, R. P. Joshi, N. P. Adhikari and U. Schwingenschlögl, *Appl. Phys. Lett*., 2014, **104**, 073116(1-5).
46. B. Chan and W.-L. Yim, *J. Chem. Theory Comput*., **9**, 2013, 1964.
47. U. Sarkar, J. Padmanabhan, R. Parthasarathi, V. Subramanian and P. K. Chattaraj, *J. Mol. Struct. (Theochem.)*, 2006, **758**, 119.
48. P. K. Chattaraj and U. Sarkar, *Int. J. Quantum Chem*., 2003, **91**, 633.
49. U. Sarkar, M. Khatua and P. K. Chattaraj, *Phys. Chem. Chem. Phys*., 2012, **14**, 1716.
50. K. B. Wiberg, *Tetrahedron*, 1968, **24**, 1083.
51. J. Deb, D. Paul, U. Sarkar and P. W. Ayers, *J. Mol. Model*., 2018, **24**, 249(1-11).
52. M. Khatua, S. Pan and P. K. Chattaraj, *J. Chem. Phys*., 2014, **140**, 164306(1-11).
53. D. Cremer and E. Kraka, *Angew. Chem*., 1984, 96, 612; *Angew. Chem*., *Int. Ed. Engl*., 1984, **23**, 627.
54. M. Ghara, S. Pan, J. Deb, A. Kumar, U. Sarkar and P. K. Chattaraj, *J. Chem. Sci*., 2016, **128**, 1537.